Anisotropy of the elastic and nonlinear acoustic properties of dense textured $Bi_2Sr_2CaCu_2O_{8+y}$

G. A. Saunders, Chang Fanggao, Li Jiaqiang, Q. Wang, M. Cankurtaran,* E. F. Lambson, P. J. Ford, and D. P. Almond

Schools of Physics and Materials Science, University of Bath, Claverton Down, Bath BA2 7AY, United Kingdom

(Received 23 August 1993)

A description of the anisotropy of elastic and nonlinear acoustic properties of dense (95% of theoretical), highly textured, sinter-forged, ceramic $Bi_2Sr_2CaCu_2O_{8+y}$ (Bi-2:2:1:2) high-T_c superconductors is provided from measurements of the velocities of longitudinal and shear ultrasonic waves as functions of temperature and hydrostatic pressure. A high proportion of the grains are aligned preferentially with the c axis along the forging direction in this material, while it is essentially isotropic in the plane normal to the forging axis. A complete set of the elastic stiffness tensor components has been determined as a function of temperature from 10 to 290 K, treating this material as if it had cylindrical symmetry. The results are used to compute the orientation dependences of the Young's modulus and Poisson's ratio which are compared with those estimated for single crystal Bi-2:2:1:2. The main finding is a marked anisotropy of the elastic stiffness moduli and their dependences on pressure. The elastic and nonlinear acoustic properties of the textured and single-crystal Bi-2:2:1:2 comply with the behavior expected for a layerlike material with rather weak interlayer binding forces: $C_{11} > C_{33}$, the linear compressibility and thermal expansion along to the c axis, i.e., normal to the layers, being substantially larger than in the ab plane. The hydrostatic pressure derivative $(\partial C_{33}/\partial P)_{P=0}(=21.3)$ of the elastic stiffness tensor component, which corresponds to a longitudinal wave propagated along the c axis, is larger than that $(\partial C_{11}/\partial P)_{P=0}(=15.1)$, for such a wave propagated in the ab plane. The anisotropies of the linear compression and the acoustic mode Grüneisen parameters are also typical of a layerlike material.

I. INTRODUCTION

The high-T_c cuprate superconductors are layerlike materials which can be expected to show highly anisotropic elastic and nonlinear acoustic properties. Due to their chemical nature and the configuration of their phase diagrams, these materials are usually made by a sintering process as polycrystalline ceramics. As it is extremely difficult to make large, defect-free single crystals, it is likely that polycrystalline materials will be the basis of many commercial applications in the foreseeable future. Hence, there is a need for a comprehensive experimental description of the materials properties of granular high-T_c superconductors, including the extent to which their elastic and nonlinear acoustic properties can be anisotropic.

One of the high-T_c superconductors which has aroused interest, particularly for potential applications, is the Bi-2:2:1:2 phase of bismuth cuprates, which has the ideal composition $Bi_2Sr_2CaCu_2O_{8+y}$ and a T_c of about 90 K.[1] Bi-2:2:1:2 has an orthorhombic crystal structure with $c(=30.8445$ Å) much larger than the lattice parameters $a(=5.4091$ Å) and $b(=5.4209$ Å) which are almost equal.[2] Compounds in the series $Bi_2Sr_2Ca_{n-1}Cu_nO_{4+2n}$, including the Bi-2:2:1:2 phase with $n=2$, have layer structures containing adjacent pairs of BiO planes that alternate along the c axis with perovskitelike multilayers. In Bi-2:2:1:2 the perovskitelike multilayer comprises two copper-oxygen sheets in the form of corner-sharing CuO_5 pyramids separated on the base sides by calcium ions.[3] The Bi_2O_2 layers consist of two parallel, planar BiO sheets. The bismuth ion coordination is six: four O in the BiO plane, one O on the adjacent BiO layer and one O on the adjacent apex of a CuO_5 pyramid. These BiO_6 octahedra are strongly distorted, having the typical oxygen coordination for Bi^{3+} with three short Bi-O bonds and three much longer Bi-O bonds in the direction of the lone pair electrons. These lone pairs are positioned in the interstice between the pairs of BiO layers leading to a large (about 3 Å) interlayer spacing.[4] Crystallites of these compounds cleave readily between these layers: interlayer binding forces appear to be weak. If this is so, the velocity of a longitudinal ultrasonic wave propagated along the c-axis direction should be much slower than that in the normal direction and this is found.[5–11]

The present objective has been to study the elastic anisotropy of dense (95% of theoretical density), highly textured, ceramic specimens of Bi-2:2:1:2. To do this, ultrasonic wave velocity measurements have been made in a number of propagation directions as a function of temperature between 10 and 290 K. The results have been used to determine the elastic stiffness components and the elastic anisotropy of this material (treating it as being cylindrically symmetric), including details of technologically important parameters such as the bulk and Young's moduli and Poisson's ratio. In addition, the effects of hydrostatic pressure on the ultrasonic mode velocities have been measured at room temperature. The pressure derivatives $(\partial C_{IJ}/\partial P)_{P=0}$ of elastic stiffnesses have been used to calculate the linear and volume compressions and the long-wavelength acoustic mode Grüneisen parameters. Since the elastic moduli of ceramics, and especially their pressure dependences, are sensitive to their porous nature, one must be careful in deciding whether the ob-

served pressure effects are intrinsic or due to the microstructure (particularly porosity, microcracks, and grain boundaries) of these granular materials. To appraise the influence of the microstructure, the results obtained for the dense, textured Bi-2:2:1:2 are compared with the data available from ultrasonic[6,10] and Brillouin scattering studies[7] of monocrystalline Bi-2:2:1:2.

II. EXPERIMENTAL PROCEDURES

The samples were made at Argonne National Laboratory by the sinter-forging method described previously.[8] The specimen structure was characterized by x-ray-diffractometry analysis.[11] Strong (001) plane reflections were observed from the top face of a sample. When the x rays were incident on the two side faces, these particular reflection peaks were almost absent and different reflections, such as that from the (200) plane, become prominent. These results established the textured nature of the samples: a high proportion of the grains are aligned preferentially with the c axis perpendicular to the top face of the specimens, that is along the forging direction. In addition the reflection peaks from the two side faces were very similar in both position and intensity, showing that the sample is essentially isotropic in the plane parallel to the top and bottom faces. The sample density, determined by Archimedes' principle using acetone as the flotation liquid, was 6210 kg m^{-3} which is about 95% of the x-ray density.

The samples were cut in the form of rectangular parallelepipeds and polished lightly to give flat and parallel faces to about 10^{-4} rad. One pair of sample faces was perpendicular to the forging direction, which was virtually the c axis of the individual grains. To generate and detect ultrasonic pulses, X- or Y-cut (for longitudinal and shear waves, respectively) quartz 10-MHz transducers were bonded to the specimen using Nonaq stopcock grease for temperature studies and Dow resin for pressure studies. The effects of temperature and pressure on ultrasonic wave transit time were measured using a pulse-echo overlap system,[12] capable of detecting changes in ultrasonic transit time to 1 part in 10^5. A transducer correction[13] was applied to the measured transit time and, in turn, to the ultrasonic wave velocities. The hydrostatic pressure dependence up to 0.15 GPa of the sound velocity was measured at room temperature (290 K) in a piston and cylinder apparatus using silicone oil as the pressure-transmitting medium. Pressure was measured with a precalibrated manganin resistance gauge. Pressure-induced changes in the sample dimensions were accounted for by using the "natural velocity (W)" technique.[14]

III. THE ELASTIC STIFFNESS TENSOR OF TEXTURED Bi-2:2:1:2

To model the anisotropy of the elastic and nonlinear acoustic properties of this polycrystalline material comprised of orthorhombic platelike crystallites arranged largely with the c axis along one direction, but oriented at random in the ab plane, it is treated as if it had cylindrical symmetry. In this case there are five independent components of the corresponding elastic stiffness tensor which can be represented in matrix form in Voigt notation by

$$\begin{vmatrix} C_{11} & C_{12} & C_{13} & 0 & 0 & 0 \\ C_{12} & C_{11} & C_{13} & 0 & 0 & 0 \\ C_{13} & C_{13} & C_{33} & 0 & 0 & 0 \\ 0 & 0 & 0 & C_{44} & 0 & 0 \\ 0 & 0 & 0 & 0 & C_{44} & 0 \\ 0 & 0 & 0 & 0 & 0 & C_{66} \end{vmatrix} , \tag{1}$$

where C_{66} is equal to $(C_{11}-C_{12})/2$. *It is important to note that the C_{IJ} here do not refer to the elastic stiffness tensor components of the orthorhombic crystal itself.* For a direction, specified by the direction cosines n_1, n_2, and n_3, three bulk waves can be propagated with velocities (V) and polarizations (u_k) determined by the Christoffel equations

$$(L_{ik}-\rho V^2\delta_{ik})u_k=0 \quad (i,k=1,2,3) . \tag{2}$$

The Christoffel coefficients for this symmetry are given by

$$L_{11}=n_1^2C_{11}+n_2^2C_{66}+n_3^2C_{44} , \tag{3}$$

$$L_{22}=n_1^2C_{66}+n_2^2C_{11}+n_3^2C_{44} , \tag{4}$$

$$L_{23}=n_2n_3(C_{13}+C_{44}) , \tag{5}$$

$$L_{33}=n_1^2C_{44}+n_4^2C_{44}+n_3^2C_{33} , \tag{6}$$

$$L_{12}=n_1n_2(C_{12}+C_{66}) , \tag{7}$$

and

$$L_{13}=n_1n_3(C_{13}+C_{44}) . \tag{8}$$

The velocities of eight ultrasonic modes have been measured as a function of temperature and pressure in the textured Bi-2:2:1:2. The mode configurations and the ultrasonic wave velocities measured at room temperature and atmospheric pressure are presented in Table I. Only five of the eight velocities are needed to determine all the elastic stiffnesses specified in the cylindrical model. The following relationships, obtained by solution of the

TABLE I. Mode configurations and velocities of 10-MHz ultrasonic waves propagated in textured Bi-2:2:1:2 at 290 K. The Miller indices correspond to a structure of cylindrical symmetry.

Mode	Direction of propagation	Direction of polarization	Velocity (m s^{-1}) (±10)
1	[001]	[001]	2670
2	[001]	In the (001) plane	1750
3	[100]	[100]	4370
4	[100]	[010]	2460
5	[100]	[001]	1740
6	[0,$2^{-1/2}$,$2^{-1/2}$]	[0,0.95,0.30]	3430
7	[0,$2^{-1/2}$,$2^{-1/2}$]	[0,0.31,−0.95]	2155
8	[0,$2^{-1/2}$,$2^{-1/2}$]	[100]	2150

Christoffel equations, between the ultrasonic velocities (for the modes listed in Table I) and elastic stiffness tensor components, can be used to obtain C_{IJ}:

$$\rho V_1^2 = C_{33} , \tag{9}$$

$$\rho V_2^2 = C_{44} , \tag{10}$$

$$\rho V_3^2 = C_{11} , \tag{11}$$

$$\rho V_4^2 = C_{66} , \tag{12}$$

$$\rho V_5^2 = C_{44} , \tag{13}$$

$$\rho V_6^2 = \tfrac{1}{4}(C_{11}+C_{33})+\tfrac{1}{2}C_{44} + \tfrac{1}{4}[(C_{11}-C_{33})^2+4(C_{13}+C_{44})^2]^{1/2} , \tag{14}$$

$$\rho V_7^2 = \tfrac{1}{4}(C_{11}+C_{33})+\tfrac{1}{2}C_{44} - \tfrac{1}{4}[(C_{11}-C_{33})^2+4(C_{13}+C_{44})^2]^{1/2} , \tag{15}$$

$$\rho V_8^2 = \tfrac{1}{2}(C_{44}+C_{66}) . \tag{16}$$

The mode velocities V_1, V_2, V_3, V_4, and V_6 have been used to calculate the five elastic stiffness tensor components. Complete sets of the elastic stiffness tensor components C_{IJ} and elastic compliances S_{IJ} obtained at 290 and 20 K are given in Table II (top). The other three modes were used previously[11] to test the validity of the assumption of a structure of cylindrical symmetry. For a cylindrical structure, it would be expected that

$$\rho V_5^2 = \rho V_2^2 = 19 \text{ GPa} ,$$

$$\rho V_8^2 = \tfrac{1}{2}(C_{44}+C_{66}) = \tfrac{1}{2}(\rho V_2^2+\rho V_4^2) = 28.5 \text{ GPa} .$$

The corresponding measured values are 19 and 29 GPa in very good agreement with those expected from a material of cylindrical symmetry. The velocities V_7 and V_8 of the shear and quasishear waves propagated in the direction of 45° to the c axis are very similar (Table I). A calculation based on cylindrical structure requires that these two velocities are the same when ultrasonic modes are propagated in a direction of 42° to the c axis. These results evidence that the cylindrical assumption is reasonable.

TABLE II. (Top) the elastic stiffness C_{IJ} (in GPa) and compliance S_{IJ} (in 10^{-12} Pa^{-1}) tensor components in the cylindrical representation of textured Bi-2:2:1:2 at 290 and 20 K. (Bottom) Elastic stiffness tensor components (in GPa) of single-crystal Bi-2:2:1:2 at 260 K (Ref. 6) and room temperature (Ref. 7).

T (K)	C_{11}	C_{12}	C_{13}	C_{33}	C_{44}	C_{66}
290	118.5	43.1	7.3	44.2	19.0	37.7
20	124	43.7	7.5	45.2	20.2	40.2
T (K)	S_{11}	S_{12}	S_{13}	S_{33}	S_{44}	S_{66}
290	9.77	−3.50	−1.03	23.0	52.7	26.5
20	9.24	−3.19	−1.00	22.5	49.5	24.9

Reference	C_{11}	C_{12}	C_{13}	C_{22}	C_{33}	C_{44}	C_{66}
6	130	72		110			51
7	125	79	56		76	16	

It is difficult to grow a sufficiently large, defect-free single-crystal of Bi-2:2:1:2 for accurate ultrasonic wave velocity measurements; the short-pulse transit times associated with small dimensions hinder precision measurement of elastic stiffness tensor components. Single-crystal samples are usually in the form of thin platelets; for instance, the single-crystal Bi-2:2:1:2 sample used for ultrasonic measurements by Wu *et al.*[10] was an irregular platelet with maximum dimensions $5\times4\times1.5$ mm^3 in the a, b, and c directions. Hence, complete sets of the elastic stiffness tensor components for this orthorhombic material are not yet available, although partial sets are [Table II (bottom)]. Anisotropic elastic properties were found in the ab plane: the velocities of longitudinal modes propagated along the a axis and b axis were reported[10] as 4320 and 4097 m s^{-1}, respectively, leading to the difference observed between C_{11} and C_{22}. Due to the small size along the c-axis direction of the platelet, C_{33} has not been measured for single-crystal Bi-2:2:1:2 by ultrasonic techniques.[6,10] However, Brillouin scattering measurements,[7] have established a large difference between the sound velocities in the ab plane and along the c axis: $C_{11} > C_{33}$. Comparison between the data given in Table II shows that the elastic stiffnesses C_{11} and C_{44} are similar for both the textured ceramic and monocrystalline Bi-2:2:1:2. However, the other moduli, especially C_{13}, are substantially smaller for the textured ceramic than for the crystalline material.

The in-plane longitudinal velocity (=4370 m s^{-1}) measured for textured Bi-2:2:1:2 (see Table I) is in excellent agreement with that obtained for single-crystal (platelet) samples obtained using ultrasonic pulse-echo[6,10] and Brillouin light scattering[7] techniques. The high longitudinal velocity value observed in the ab plane, compared with that in the c axis, for textured Bi-2:2:1:2 (Table I) and the cognisance that $C_{33} < C_{11}$ (Table II) establishes that the elastic stiffness within the ab layers is large compared with the binding forces between layers.

The velocity (=2670 m s^{-1}) of the longitudinal ultrasonic waves propagated along the c-axis direction of textured Bi-2:2:1:2 is much slower than that (=3413±212 m s^{-1}) measured along the c axis of single-crystal (platelet) Bi-2:2:1:2 samples using Brillouin light scattering,[7] whereas the transverse velocities measured for both textured and single-crystal Bi-2:2:1:2 samples are in reasonable agreement. This implies that the observed difference between the velocities of longitudinal sound waves propagated along the c-axis directions of textured and single-crystal Bi-2:2:1:2 samples is not due solely to porosity and microcracking but may result in part from reduction in velocity of the longitudinal sound waves propagated along the "c-axis" direction in a loosely stacked material comprised of weakly adhering platelike grains.

In general, the elastic stiffnesses of the high-temperature superconducting cuprate ceramics, especially for the bismuth-based materials, are small. Measurements made on sintered Bi-2:2:1:2 ceramics by several different research groups (for a review see Ref. 15) have shown that the ultrasonic wave velocities are slow with a longitudinal velocity of about 2900±400 m s^{-1} and a transverse velocity of 2000±300 m s^{1}—substantially less

than might be expected from average values of the single-crystal velocity data. A useful parameter for a comparison is the bulk modulus B^S. In the absence of a complete set of elastic stiffness tensor components, it is not possible to calculate a definitive bulk modulus for monocrystalline Bi-2:2:1:2. However, using the elastic stiffness moduli [Table II (bottom)] determined by Brillouin scattering experiments[7] and assuming a structure of cylindrical symmetry leads to a estimated value of 70 GPa for the bulk modulus of single-crystal Bi-2:2:1:2. Yoneda *et al.*[16] obtained a value of 61 GPa for the bulk modulus of Bi-2:2:1:2 from very high-pressure x-ray-diffraction measurements of lattice parameters in a diamond cell. These values are much larger than that (31.9 GPa) obtained for the textured material (Table III). The reduced stiffness of the textured ceramic is probably due to the microstructural effects including porosity and granularity.[17] Mechanical properties studies performed recently by Goretta *et al.*[18] on dense, highly textured Bi-2:2:1:2, prepared by a similar route, indicate that the strength of highly textured bulk Bi-Sr-Ca-Cu-O superconductors is relatively low.

The bulk modulus of Bi-2:2:1:2 is much smaller than those of $YBa_2Cu_3O_{7-x}$ and $La_{1.85}Sr_{0.15}CuO_4$. One reason for this could be the strongly enhanced compressibility of the Bi_2O_2 double layer in the c direction.

TABLE III. The linear compressibilities β_{ab}^S and β_c^S and the volume compressibility β_0^S (in units of $10^{-11}\,Pa^{-1}$), the bulk modulus B^S (in units of GPa), and Poisson's ratio ν_{ij} of textured Bi-2:2:1:2 ceramic from 290 to 20 K.

T (K)	β_{ab}^S	β_c^S	β_0^S	B^S	ν_{31}	ν_{12}	ν_{13}
290	0.525	2.089	3.139	31.86	0.045	0.358	0.106
280	0.524	2.086	3.134	31.91	0.045	0.356	0.106
270	0.523	2.085	3.132	31.93	0.045	0.357	0.105
260	0.523	2.085	3.130	31.95	0.044	0.357	0.104
250	0.522	2.083	3.127	31.98	0.044	0.357	0.103
240	0.522	2.081	3.125	32.00	0.043	0.356	0.102
230	0.523	2.081	3.126	31.99	0.042	0.355	0.101
220	0.522	2.079	3.123	32.03	0.042	0.354	0.100
210	0.520	2.073	3.113	32.12	0.043	0.352	0.102
200	0.521	2.074	3.116	32.10	0.042	0.352	0.100
190	0.521	2.075	3.117	32.09	0.041	0.351	0.099
180	0.516	2.067	3.099	32.27	0.043	0.350	0.103
170	0.514	2.061	3.089	32.38	0.044	0.349	0.106
160	0.513	2.062	3.089	32.38	0.044	0.349	0.105
150	0.512	2.057	3.080	32.46	0.045	0.348	0.108
140	0.510	2.056	3.076	32.51	0.045	0.347	0.108
130	0.509	2.053	3.071	32.56	0.045	0.347	0.109
120	0.509	2.053	3.071	32.57	0.045	0.347	0.109
110	0.508	2.052	3.068	32.59	0.045	0.346	0.109
100	0.507	2.049	3.062	32.66	0.046	0.346	0.111
90	0.506	2.048	3.060	32.68	0.046	0.346	0.111
80	0.506	2.047	3.058	32.70	0.046	0.345	0.111
70	0.506	2.048	3.061	32.67	0.045	0.346	0.109
60	0.506	2.047	3.059	32.69	0.045	0.345	0.109
50	0.506	2.047	3.059	32.69	0.045	0.345	0.109
40	0.506	2.047	3.059	32.69	0.044	0.345	0.108
30	0.505	2.045	3.056	32.72	0.045	0.345	0.108
20	0.505	2.045	3.055	32.73	0.045	0.345	0.108

IV. ANISOTROPY OF THE ELASTIC BEHAVIOR OF TEXTURED Bi-2:2:1:2

To compare the elastic anisotropy of textured ceramic and monocrystalline samples of Bi-2:2:1:2, cross sections of the three wave velocity surfaces have been computed as the eigenvalues of Christoffel equations. Results obtained at room temperature for propagation directions in the (010) plane are plotted in Fig. 1. The Miller indices refer to the cylindrical approximation and not to the crystallographic axial reference frame of an orthorhombic single crystal. These velocity surface cross sections depict clearly the anisotropy in the *ac* plane. In general, the elastic behaviors of both single-crystal and textured Bi-2:2:1:2 conform with that expected for a layerlike material: the longitudinal elastic stiffness within the layers being substantially larger than that normal to the layers. The velocity of a longitudinal elastic wave transmitted within the layers is much greater than that of a wave transmitted along the direction of weak binding, namely,

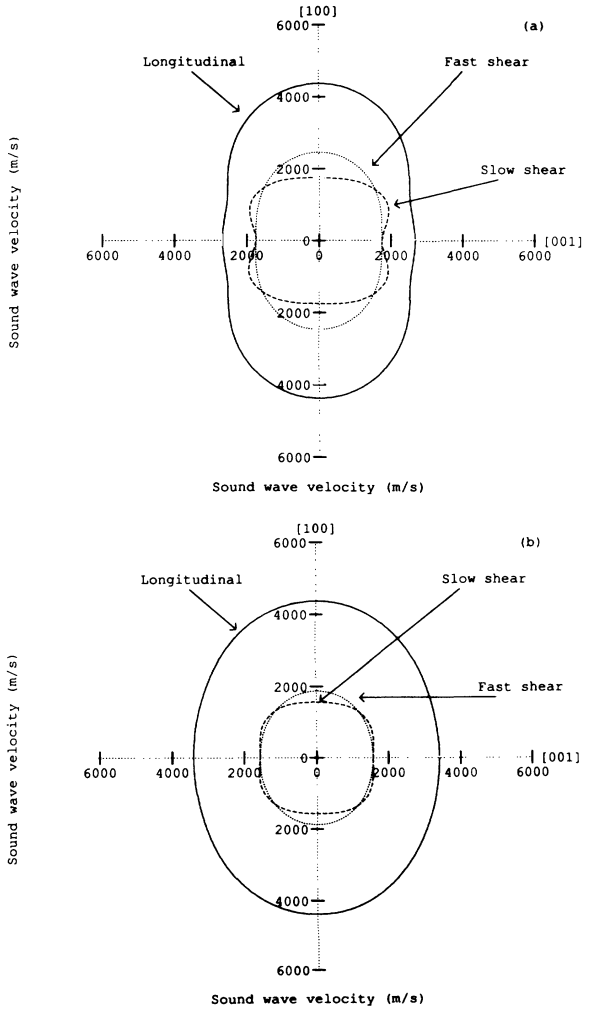

FIG. 1. (010) plane cross sections of the wave velocity surface at 290 K for (a) textured ceramic and (b) monocrystalline Bi-2:2:1:2. The solid, dotted, and dashed lines correspond to the longitudinal, fast shear, and slow shear modes, respectively.

the c axis [Fig. 1(a)]. Hence, C_{11} is much bigger than C_{33} [Table II (top)]. It is probable that the strong interatomic binding forces within the CuO layers are responsible for the ab-plane rigidity and therefore control the wave propagation within this plane so that these waves have velocities which are essentially independent of direction, i.e., C_{11} is nearly equal to C_{22} [see Table II (bottom)].

A measure of the property that, under hydrostatic pressure, the layers close up substantially while the change in the interatomic distances in a layer is much smaller, is given by the linear compressibility β. The linear compressibilities along the c direction $\beta_c^S(=2S_{13}+S_{33})$ and in the ab plane $\beta_{ab}^S(=S_{11}+S_{12}+S_{13})$ have been calculated as a function of temperature (Table III) using the elastic compliances measured for textured Bi-2:2:1:2: β_c^S is about four times larger than β_{ab}^S. This material has a markedly anisotropic response to hydrostatic pressure, contracting about four times more in the c direction than in directions in the ab plane. Thus, the effect of hydrostatic pressure is to decrease the c spacing more than that in the ab plane. From very high-pressure x-ray-diffraction measurements of lattice parameters in a diamond anvil cell Yoneda *et al.*[16] found such anisotropy for powdered Bi-2:2:1:2: the linear compressibility along the c axis direction was two times larger than that along the a axis. However, although the linear compressibility in the ab plane determined for textured Bi-2:2:1:2 is in reasonable agreement with that ($=0.43\times10^{-11}$ Pa^{-1}) obtained by Yoneda *et al.*,[16] the linear compressibility along the c axis of textured Bi-2:2:1:2 is much larger than that ($=0.83\times10^{-11}$ Pa^{-1}) found in Ref. 16. This difference can partially be attributed to the weak adhesion between the platelike grains in the textured material. Neutron-diffraction studies[19] have shown that Bi-2:2:1:2 has a strongly anisotropic thermal expansion: $\alpha_{33}(=21.7\times10^{-6}$ K$^{-1})$ along the c axis is larger than $\alpha_{11}(=14.5\times10^{-6}$ K$^{-1})$ and $\alpha_{22}(=14.8\times10^{-6}$ K$^{-1})$. These linear compressibility and thermal expansion results are in accord with the fact that in anisotropic materials the lattice vibrations are more easily excited in the softer direction.[20] As the temperature is raised the lower-energy vibrations in the more weakly bound direction are excited first so that α_{33} is larger than α_{11}.

Knowledge of the set of elastic stiffness tensor components enables determination of the material response to any applied stress system. A particularly useful visualization of the elastic anisotropy can be gained from Young's modulus surface, which depicts the ratio of the longitudinal stress to longitudinal strain as a function of orientation. For a stress applied in a given direction (with direction cosines l_1, l_2, and l_3), Young's modulus (E) for this cylindrical representation is given by

$$1/E=(l_1^4+l_2^4)S_{11}+l_3^4S_{33}+l_1^2l_2^2(2S_{12}+S_{66}) +l_3^2(1-l_3^2)(2S_{13}+S_{44}) . \quad (17)$$

Cross sections of Young's modulus surface in the (100) plane are plotted for the textured and monocrystalline Bi-2:2:1:2 in Fig. 2. Along the c axis ($l_1=l_2=0$, $l_3=1$) and the a axis ($l_1=1$, $l_2=l_3=0$) Young's modulus reduces to $1/S_{33}$ and $1/S_{11}$, respectively; since S_{33} is larger than S_{11} [Table II (top)], Young's modulus along the c axis is proportionally smaller than that in the ab plane [Figs. 2(a) and 2(b)]: the strain produced by a given stress is greater along the c axis than along the a axis. For a stress applied in the (001) plane ($l_3=0$), Eq. (17) reduces to

$$1/E=S_{11}-2[(S_{11}-S_{12})-\tfrac{1}{2}S_{66}](l_1^2l_2^2) . \quad (18)$$

In the cylindrical representation the cross section of Young's modulus surface in the (001) plane is a circle.

The value of 101 GPa determined for Young's modulus in the ab plane of textured Bi-2:2:1:2 at room temperature can be compared with that calculated from the single-crystal elastic moduli given in Table II (bottom) and that (about 70 GPa) estimated[21] for the in-plane Young's modulus of Bi-2:2:1:2 single crystal from vibrating reed measurements at kHz frequencies. Young's moduli of both textured and single-crystal Bi-2:2:1:2 samples are much larger than that (about 25 GPa) found for sintered Bi-2:2:1:2 ceramics using ultrasonic techniques.[22] They are also much larger than that for the in-plane Young's modulus obtained from static stress versus strain curves for single-crystal Bi-2:2:1:2 whiskers: 20±5 GPa at 270 K,[23] 27 GPa at room temperature (an average over 53 samples).[24] It has been suggested that the presence of grain boundaries lowers substantially the elastic modulus.[24]

Poisson's ratio ν_{ij} is given by the ratio of the lateral (ε_{jj}) to longitudinal (ε_{ii}) strain resulting from a longitudinal stress:

$$\begin{aligned}\nu_{ij}&=-\varepsilon_{jj}/\varepsilon_{ii}=-S_{jjii}\sigma_{ii}/S_{iiii}\sigma_{ii}\\&=-S_{jjii}/S_{iiii}=-S_{iijj}/S_{iiii}\\&=-S_{IJ}/S_{II}\\&\qquad(I,J=1,2,3,\ I\neq J) . \quad (19)\end{aligned}$$

In normal engineering usage of isotropic materials a positive longitudinal strain is always accompanied by a negative lateral strain, the negative sign in the definition ensures that Poisson's ratio is positive. For an anisotropic material, Poisson's ratio depends upon the direction of the applied stress, hence

$$\nu_{ij}=-S'_{iijj}/S'_{iiii} , \quad (20)$$

where the prime notation corresponds to transformation to a new axial set x', y', z'. If the stress is applied along x', then Poisson's ratio ν_{12} is $-S'_{1122}/S'_{1111}$, where the values of S'_{1111} and S'_{1122} can be obtained using the transformation

$$S'_{ijkl}=a_{im}a_{jn}a_{kp}a_{lq}S_{mnpq} . \quad (21)$$

The direction cosines a_{ij} can be found by the method of Eulerian angles.[25,26] The required expressions for the transformed elastic compliance constants S'_{11} and S'_{12} are

$$\begin{aligned}S'_{11}&=(a_{11}^4+a_{12}^4)S_{11}+2a_{11}^2a_{12}^2S_{12}\\&\quad+2a_{13}^2(1-a_{13}^2)S_{13}+a_{13}^4S_{33}\\&\quad+a_{13}^2(1-a_{13}^2)S_{44}+a_{11}^2a_{12}^2S_{66} \quad (22)\end{aligned}$$

and

$$S'_{12}=(a_{11}^2a_{21}^2+a_{12}^2a_{22}^2)S_{11}+(a_{21}^2a_{12}^2+a_{11}^2a_{22}^2)S_{12}+[a_{23}^2(a_{11}^2+a_{12}^2)+a_{13}^2(a_{21}^2+a_{22}^2)]S_{13}+a_{23}^2a_{13}^2S_{33}+a_{13}a_{23}(a_{12}a_{22}+a_{11}a_{21})S_{44}+a_{21}a_{22}a_{11}a_{12}S_{66}\ . \quad (23)$$

Poisson's ratio has been calculated in planes perpendicular to a number of selected applied stress directions. The results obtained at 290 K for the textured ceramic and single-crystal Bi-2:2:1:2 are compared in Fig. 3. In the (001) plane Poisson's ratio is isotropic: the lateral strain incurred by application of a longitudinal stress along the [001] direction is the same in all directions in this plane (this is a consequence of the identity $S'_{13}=S'_{23}=S_{13}$ in the cylindrical representation). The other curves in Fig. 3 show how Poisson's ratio varies in planes normal to the direction of applied stress. Poisson's ratio is almost independent of temperature (Table III). A value of 0.164 has been estimated for the mean Poisson's ratio of textured Bi-2:2:1:2 at room temperature.

V. THE TEMPERATURE AND PRESSURE DEPENDENCES OF THE ELASTIC STIFFNESSES OF TEXTURED Bi-2:2:1:2

The temperature dependences of elastic stiffness tensor components of the textured Bi-2:2:1:2 in the cylindrical representation are shown in Fig. 4. The data for each component fall on a smooth curve and are continuous. Neither the temperature dependences of the velocity for all the modes nor the elastic stiffness tensor components show the anomalous steplike changes and hysteresis observed by several groups in sintered bismuth-based cuprates (see Ref. 22). In recent measurements on monocrystalline samples, phonon softening for the in-plane shear mode of Bi-2:2:1:2 has been reported.[10] For the textured ceramic there are no indications of phonon soften-

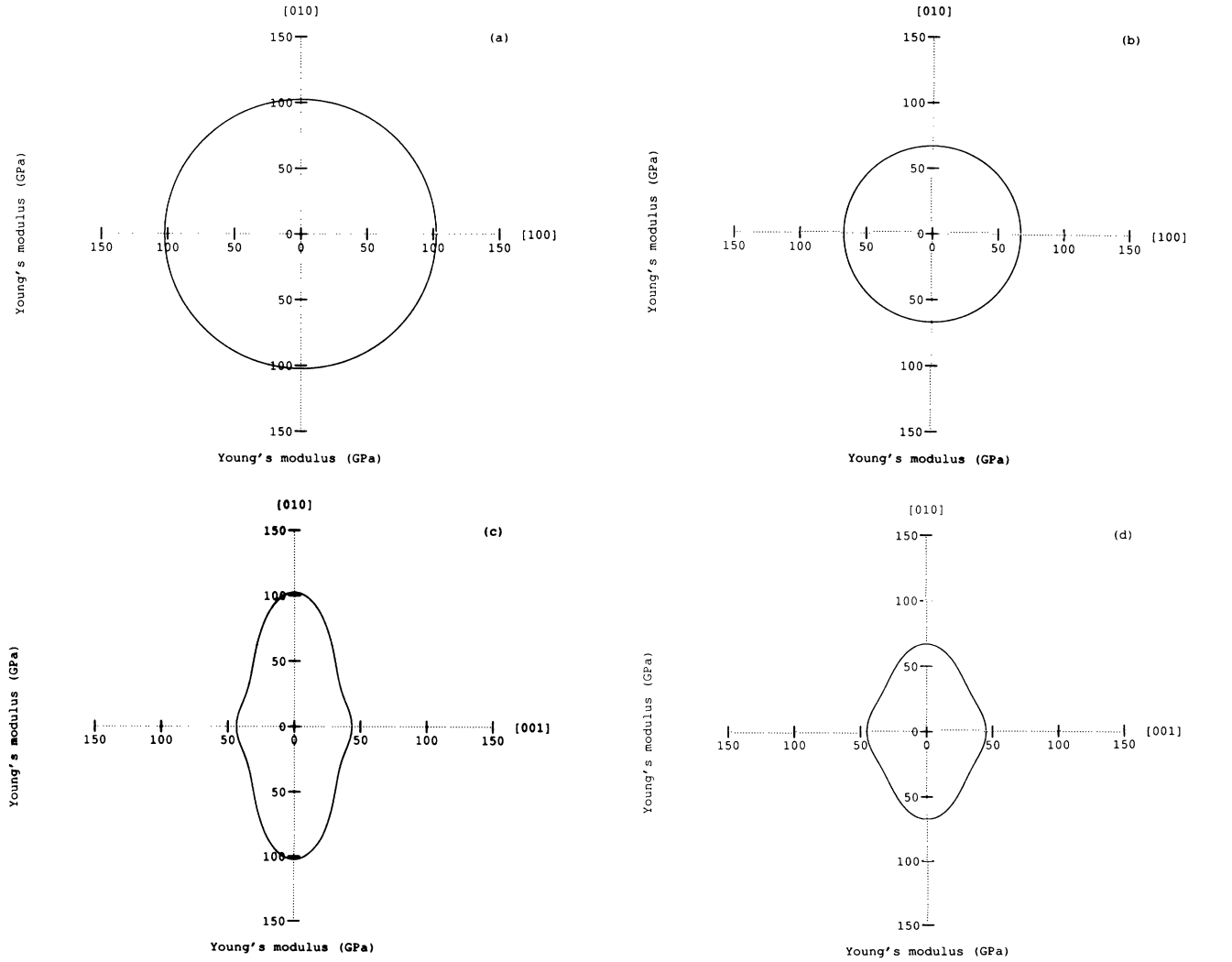

FIG. 2. (001) and (100) plane cross sections of Young's modulus surfaces at 290 K for (a and c) textured ceramic and (b and d) monocrystalline Bi-2:2:1:2.

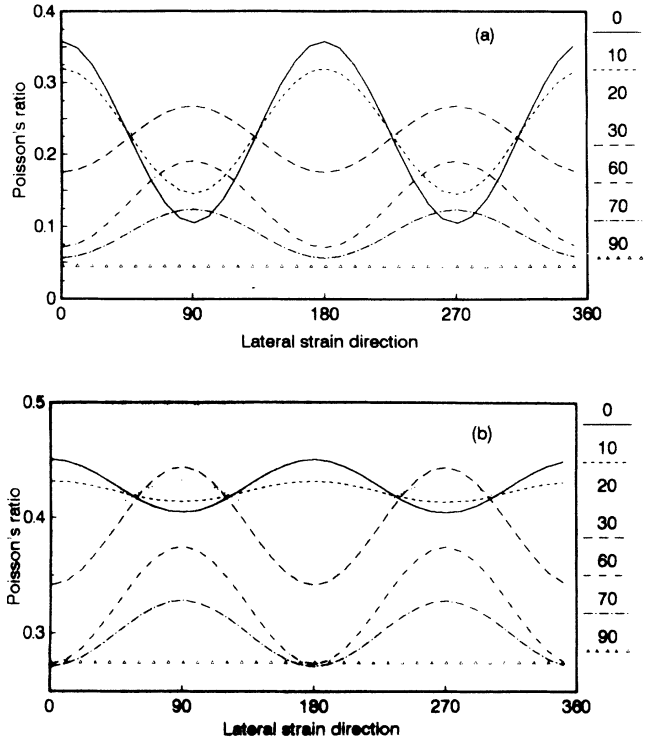

FIG. 3. The dependence of Poisson's ratio upon the direction of lateral strain measured from the *b* axis in the *ab* plane for (a) textured ceramic and (b) monocrystalline Bi-2:2:1:2 at 290 K. The direction of the longitudinal stress is specified by an angle (see the nomenclature of the right-hand side of the diagram) which is measured from the *a* axis is the *ac* plane.

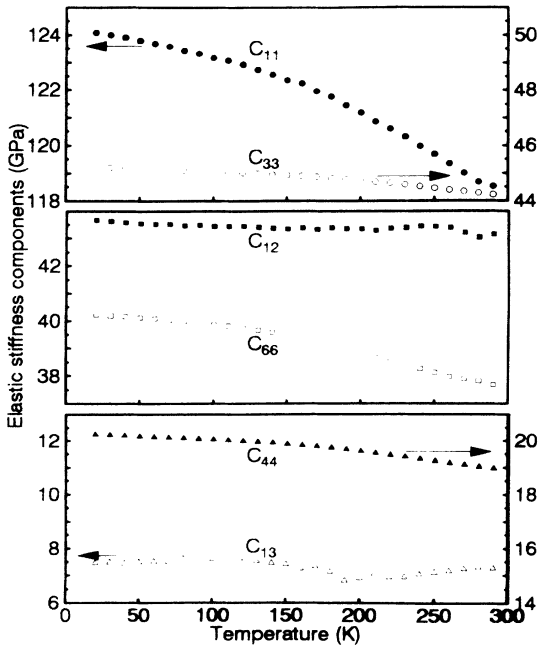

FIG. 4. The temperature dependence of the elastic stiffness tensor components C_{11}, C_{33}, C_{12}, C_{66}, C_{44}, and C_{13} of textured Bi-2:2:1:2 in the cylindrical representation.

ing. The temperature dependence of Young's and bulk moduli (Fig. 5) also show smooth behavior. No anomalies were observed in the temperature dependences of the in-plane Young's modulus[27,21] and out-of-plane shear modulus[27] of Bi-2:2:1:2 single crystal in the low-frequency vibrating reed measurement.

However, it is interesting to note that after the specimen had been recut to obtain the off-axis modes at 45° (Table I), the temperature dependences of these particular modes exhibited measurable anomalies at about 200 K, together with thermal hysteresis, an indication that they may well be associated with microstructural defects (which might be introduced by the stress applied during cuting and repolishing) and are not an intrinsic property of Bi-2:2:1:2. Recently, from static stress-strain measurements, Tritt *et al.*[28] found anomalous elastic properties in single-crystal whiskers of the Bi-2:2:1:2 material: the magnitude of Young's modulus decreased by a factor of 3–4 between 270 and 330 K and a marked hysteresis was observed in the stress-strain curves at temperatures above about 275 K. This large decrease in Young's modulus along with the presence of hysteresis were ascribed to the existence of a stress-induced phase transition. The anomalous temperature dependence of Young's modulus was absent in the vibrating reed measurements made by the same group on the single-crystal whiskers of Bi-2:2:1:2.[28] This finding seems to imply that the anomalies observed in the temperature dependence of elastic moduli of these layered materials depend on the magnitude of the applied or residual stress.

The phonon distribution of a material such as Bi-2:2:1:2, which contains a large number (60) of atoms per unit cell, includes a large number of optic branches. The elastic stiffness measurements enable only the acoustic phonon density of states to be modeled by a Debye distribution—the excluded optic modes can then be treated separately. The method of integrating over the velocity space has been used to obtain the Debye temperature Θ_D^{el} from the elastic stiffness moduli:

$$\Theta_D^{el} = \left[\frac{9n}{4\pi}\right]^{1/3}\left[\frac{h}{k}\right]\left[\int\left[\frac{1}{V_j^3}+\frac{1}{V_k^3}+\frac{1}{V_l^3}\right]\frac{d\Omega}{\pi}\right]^{-1/3}, \tag{24}$$

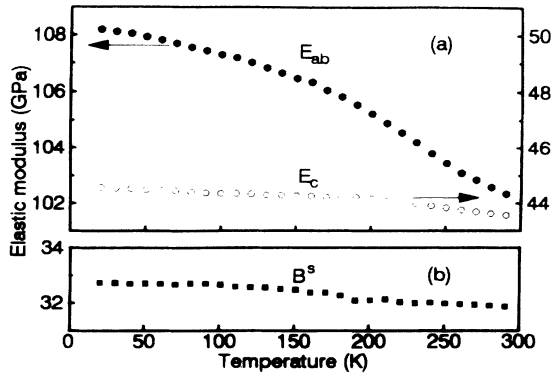

FIG. 5. The temperature dependences of (a) Young's moduli E_{ab} and E_c and (b) bulk modulus B^s of textured Bi-2:2:1:2 in the cylindrical representation.

where n corresponds to the number of atoms per unit volume. The velocities V_j, V_k, and V_l have been calculated as the eigenvalues of the Christoffel equations for each direction. The integration has been performed over the whole velocity space over equal solid angles subtending 1.218×10^{-3} sr. The calculated Debye temperature Θ_D^{el} at 20 K for Bi-2:2:1:2 is 275±6 K. From specific-heat measurements on polycrystalline specimens of Bi-2:2:1:2 Collocott and Driver[29] obtained a value of 253±7 K for the limiting Debye temperature Θ_D^0. They also reported that at temperatures above 6 K, $Bi_2Sr_2CaCu_2O_8$ shows an extremely rapid departure from simple T^3 (Debye) behavior due to dispersion from acoustic mode and the excitation of low-lying optic modes.

The effects of hydrostatic pressure on the velocities of longitudinal and shear 10-MHz ultrasonic waves propagated in the dense, textured Bi-2:2:1:2 specimens were measured at room temperature. For each mode, the measurements were reproducible and hysteresis was minimal under pressure cycling; the ultrasonic velocities increased linearly with pressure, much more steeply for the longitudinal than the shear modes (Fig. 6). The pressure derivatives $(\partial C_{IJ}/\partial P)_{P=0}$ of the elastic stiffnesses were obtained from the ultrasonic wave velocity measurements under pressure using the equation[30]

$$(\rho V^2)'_{P=0}=\rho_0 V_0^2\left[\frac{2f'}{f_0}+\chi^T-2N_kN_mS^T_{kmii}\right]_{P=0}, \quad (25)$$

where ρ_0 and V_0 are the density and the mode velocity at atmospheric pressure, χ^T $[=1/B^T=2(S^T_{11}+S^T_{12}+S^T_{13})+(2S_{13}+S^T_{33})]$ is the isothermal volume compressibility, f is the pulse echo overlap frequency at atmospheric pressure, f' is its pressure derivative, and N_k and N_m are the direction cosines of the wave propagation direction. The results for $(\partial C_{IJ}/\partial P)_{P=0}$ obtained at 290 K are summarized in Table IV. The hydrostatic pressure derivative $(\partial C_{33}/\partial P)_{P=0}$ of the elastic stiffness tensor component C_{33}, which corresponds to a longitudinal wave propagated along the c axis, is larger than that $(\partial C_{11}/\partial P)_{P=0}$ for such a wave propagated in the ab plane. This is consistent with weaker interlayer binding forces compared to the intralayer forces within the ab plane itself; since the effect of pressure causes the layers to close up substantially while decreasing the in-plane distances to a much lesser extent ($\beta_c^S>\beta_{ab}^S$), $(\partial C_{33}/\partial P)_{P=0}$ is larger than $(\partial C_{11}/\partial P)_{P=0}$. It is interesting to note that $(\partial B^S/\partial P)_{P=0}(=13.9)$ of textured Bi-2:2:1:2 is markedly smaller than that (about 21) of ceramic Bi(Pb)-2:2:1:2 prepared by the usual sintering process.[31] Olsen *et al.*[32] obtained a value of 6.0±0.3 for $BiSrCaCu_2O_x$ from very high-pressure x-ray-diffraction measurements of lattice parameters in diamond anvil cell.

In the absence of single-crystal data for the effects of pressure on the elastic stiffness tensor, it is not possible at present to separate the intrinsic from defect contributions to the $(\partial C_{IJ}/\partial P)_{P=0}$ for the textured ceramic. Pressure studies of porous ceramics have pitfalls and it is necessary to retain an awareness of the shortcomings of any interpretations. To proceed with a qualitative assessment of the anisotropy of pressure effects on the elastic properties of the textured Bi-2:2:1:2 ceramic, we will follow the stratagem of considering that the effects of defects are small, which although not strictly true, does provide a straightforward approach for determination of the compression and long-wavelength acoustic mode Grüneisen parameters.

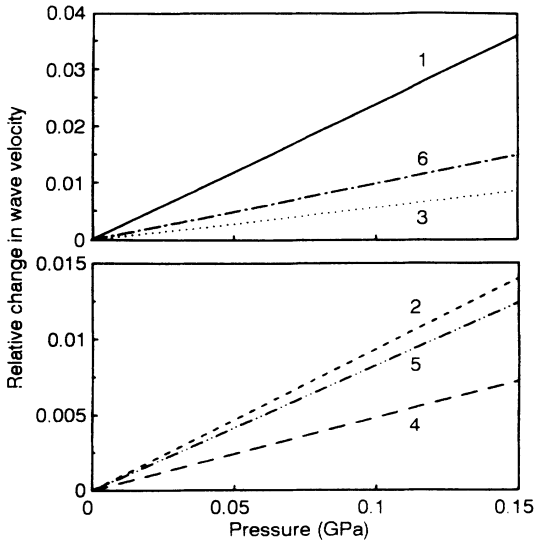

FIG. 6. Hydrostatic pressure dependences of the velocities of 10-MHz ultrasonic waves propagated in textured Bi-2:2:1:2 at 290 K. The modes are labeled as in Table I. For clarity, only the straight lines obtained from the least-squares fits to the experimental data points are shown.

VI. THE VOLUME AND LINEAR COMPRESSIONS AND THE ACOUSTIC MODE GRÜNEISEN PARAMETERS OF TEXTURED Bi-2:2:1:2

Knowledge of the compression $V(P)/V_0$ [the ratio of the volume $V(P)$ at an arbitrary pressure to that V_0 at atmospheric pressure] is useful in theoretical studies of the physical properties of a solid under pressure. The volume compression of highly textured Bi-2:2:1:2 at 290 K has been calculated up to 20 GPa (Fig. 7) by using the Murnaghan equation of state[33] in the logarithmic form

$$\ln\left[\frac{V_0}{V(P)}\right]=\frac{1}{B_0'^T}\ln\left[\frac{B_0'^T}{B_0^T}P+1\right], \quad (26)$$

TABLE IV. The hydrostatic pressure derivatives $(\partial C_{IJ}/\partial P)_{P=0}$ of the elastic stiffness tensor components of textured Bi-2:2:1:2 at 290 K in the zero-pressure limit.

$(\partial C_{11}/\partial P)_{P=0}$	$(\partial C_{12}/\partial P)_{P=0}$	$(\partial C_{13}/\partial P)_{P=0}$	$(\partial C_{33}/\partial P)_{P=0}$	$(\partial C_{44}/\partial P)_{P=0}$	$(\partial C_{66}/\partial P)_{P=0}$	$(\partial B^s/\partial P)_{P=0}$
15.1	6.7	15.4	21.3	3.4	4.2	13.9

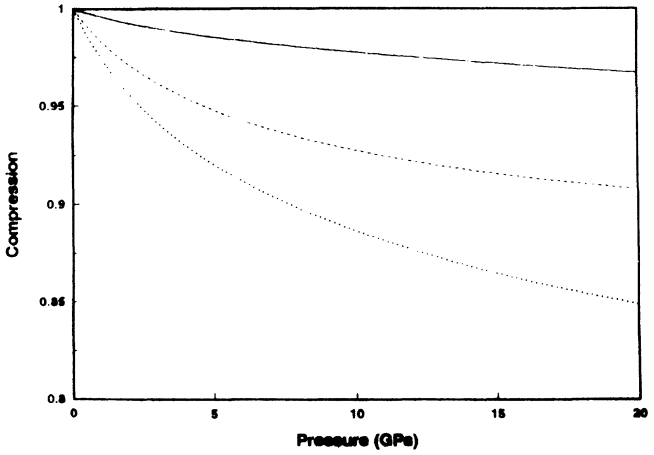

FIG. 7. The volume $V(P)/V_0$ and linear $a(P)/a_0$ and $c(P)/c_0$ compressions of textured Bi-2:2:1:2 at 290 K extrapolated to high pressure. The solid, dashed, and dotted lines correspond to $a(P)/a_0$, $c(P)/c_0$ and $V(P)/V_0$, respectively.

where B_0^T and $B_0'^T$ are the isothermal bulk modulus and its pressure derivative at zero pressure, respectively.

The changes of the linear dimensions of a solid can also be extrapolated to high pressure. Thurston[34] has given a method to estimate the lattice parameter changes under high pressure by using the ultrasonic data measured at atmospheric pressure and assuming that the pressure derivative of the bulk modulus is a constant at a given temperature. A cylindrical material has two principle stretch directions: in the *ab* plane, vertical to the *c* axis (labeled by a subscript 1), and along the *c* axis (labeled by a subscript 3). The stretch (or compression) along the *a* or *b* axis is

$$\frac{a}{a_0}=e^{(a_1+B_0^T y_1/B_0'^T)P}\left[\frac{B^T}{B_0^T}\right]^{-(B_0^T)^2 y_1/(B_0'^T)^2}, \tag{27}$$

and the stretch (or compression) along the *c* axis is

$$\frac{c}{c_0}=e^{(a_3+B_0^T y_3/B_0'^T)P}\left[\frac{B^T}{B_0^T}\right]^{-(B_0^T)^2 y_3/(B_0'^T)^2}. \tag{28}$$

Here

$$\begin{aligned} a_i&=-s_i \quad (i=1,3)\,, \\ y_1&=(S_{11}^T+S_{12}^T)Q_1+S_{13}^T Q_3\,, \end{aligned} \tag{29}$$

and

$$y_3=2S_{13}^T Q_1+S_{33}^T Q_3\,, \tag{30}$$

with

$$s_1=S_{11}^T+S_{12}^T+S_{13}^T\,, \tag{31}$$

$$s_3=2S_{13}^T+S_{33}^T\,, \tag{32}$$

$$Q_1=s_1\left[\left[\frac{\partial C_{11}}{\partial P}\right]_{T,P=0}+\left[\frac{\partial C_{12}}{\partial P}\right]_{T,P=0}\right]+s_3\left[\frac{\partial C_{13}}{\partial P}\right]_{T,P=0}, \tag{33}$$

and

$$Q_3=2s_1\left[\frac{\partial C_{13}}{\partial P}\right]_{T,P=0}+s_3\left[\frac{\partial C_{33}}{\partial P}\right]_{T,P=0}. \tag{34}$$

The linear compression in the *ab* plane has been extrapolated to 20 GPa using Eq. (27). The adiabatic quantities at 290 K have been used in the calculations since the specific heat of this material is not available. The results together with the volume compression are shown in Fig. 7. Due to the relatively large value of the hydrostatic pressure derivative $(\partial C_{33}/\partial P)_{P=0}$ (Table IV) and of the compliance S_{33} [Table II (top)], this method of extrapolation is not suitable for the linear compression along the *c* axis. Therefore, the linear compression along the *c* axis has been extrapolated up to 20 GPa by using

$$\frac{c(P)}{c_0}=\frac{V(P)}{V_0}\Big/\left[\frac{a(P)}{a_0}\right]^2. \tag{35}$$

The strong anisotropy of the linear compression is clear (Fig. 7). Of the high-T_c superconductors with perovskite-like structure, the Bi-2:2:1:2 compound is the most compressible (for a review see Ref. 35). The larger *c*-axis compressibility in Bi-2:2:1:2 has been ascribed to relatively soft BiO layers in this direction, which separate the group of CuO_2 planes. The lone-pair bond from the Bi *p* orbitals leads to particularly weak binding (bond length of 3.2 Å) between the adjacent BiO layers[36] (and relatively small C_{33}); as a result the Bi compounds cleave readily between the BiO layers.

Properties of a solid that depend upon thermal motion of the atoms are much influenced by anharmonicity, the nonlinearity of interatomic forces with respect to atomic displacements. It is usual to describe the anharmonic properties in terms of Grüneisen parameters, which quantify the volume or strain dependence of the lattice vibrational frequencies. For elastic waves the wavelength is so long that the elastic continuum model can be used to obtain the acoustic mode Grüneisen parameters. For a crystal with volume (V) changes induced by application of hydrostatic pressure, Brugger[37] introduced a Grüneisen parameter $\gamma_p(\mathbf{q})$ for the vibrational mode of wave vector $\mathbf{q}$, frequency $\omega_p(\mathbf{q})$, and polarization index p ($=1,2,3$):

$$\gamma_p(\mathbf{q})=-\left[\frac{V}{\omega_p(q)}\left[\frac{\partial\omega_p(\mathbf{q})}{\partial V}\right]_T\right]_{P=0}. \tag{36}$$

In the cylindrical representation the general relationship expressing the acoustic mode Grüneisen parameter $\gamma_p(\mathbf{q})$ of a mode in a branch of index p is related to hydrostatic pressure derivatives of the second-order elastic constants by[38]

$$\gamma_p(\mathbf{N})=\frac{-B^T}{2\omega}\{1+2\omega[(S_{11}^T+S_{12}^T+S_{13}^T)(U_1^2+U_2^2)+(2S_{13}^T+S_{33}^T)U_3^2]-B_{11}(N_1^2U_1^2+N_2^2U_2^2)$$
$$-2B_{12}N_1N_2U_1U_2-2B_{13}(N_1N_3U_1U_3+N_2N_3U_2U_3)-B_{33}N_3^2U_3^2$$
$$-B_{44}[(N_1U_3+N_3U_1)^2+(N_2U_3+N_3U_2)^2]-B_{66}(N_1U_2+N_2U_1)^2\} . \quad (37)$$

Here N_i and U_i $(i=1,2,3)$ are the direction cosines of the wave propagation and the particle displacement directions, respectively. The thermodynamic coefficients $B_{\lambda\mu}$ are related with the hydrostatic pressure derivatives $(\partial C_{IJ}/\partial P)_{P=0}$ by

$$\left[\frac{\partial C_{11}}{\partial P}\right]_{P=0}-B_{11}=-1+(s_3-2s_1)C_{11} ,$$
$$\left[\frac{\partial C_{12}}{\partial P}\right]_{P=0}-B_{12}=1+(s_3-2s_1)C_{12} ,$$
$$\left[\frac{\partial C_{13}}{\partial P}\right]_{P=0}-B_{13}=1-s_3C_{13} , \quad (38)$$
$$\left[\frac{\partial C_{33}}{\partial P}\right]_{P=0}-B_{33}=-1+(2s_1-3s_3)C_{33} ,$$
$$\left[\frac{\partial C_{44}}{\partial P}\right]_{P=0}-B_{44}=-1-s_3C_{44} ,$$
$$\left[\frac{\partial C_{66}}{\partial P}\right]_{P=0}-B_{66}=-1+(s_3-2s_1)C_{66} .$$

The acoustic mode Grüneisen parameters, calculated using Eq. (37), for the textured Bi-2:2:1:2 at 290 K are given in Fig. 8 as a function of wave propagation direction. The mode Grüneisen parameters are constant in the *ab* plane while in the *ac* or *bc* plane they vary with ultrasonic wave propagation direction as a result of the anisotropy of the material. In the *ab* plane the value of longitudinal mode Grüneisen parameter (γ_L) is smaller than that γ_{s2} for the shear mode which is polarized along the *c* axis: the vibrational anharmonicity of the longitudinal acoustic phonons is less pronounced than that of mode *S*2 shear phonons. In the *bc* plane the longitudinal mode Grüneisen parameter increases to reach its maximum value of 7.9 as the wave propagation direction approaches the *c* axis. The value of the shear mode Grüneisen parameter γ_{s1} (the polarization direction of this mode is in the *ab* plane) is always smaller than that of the longitudinal mode and also shows a small maximum when the wave propagation direction is along the *c* axis. In the *bc* or *ac* plane the anharmonicity of the shear mode *S*2, which is polarized in the *bc* or *ac* plane, reduces as the wave propagation gets closer to the *c* axis. The rapid increase of the value of γ_L in these two planes indicates that the vibrational anharmonicity is greatly enhanced for the longitudinal mode propagated along the *c* axis. Like the elastic properties, the nonlinear acoustic behavior of textured Bi-2:2:1:2 is in accord with that expected of a layerlike material with rather weak interlayer bonding. The mean acoustic mode Grüneisen parameter γ^{el} (=2.5) has been calculated by summing over the whole space Ω all of the long-wavelength acoustic mode Grüneisen parameters with the same weight for each mode. This is in good agreement with the low-temperature thermal Grüneisen parameter γ_0^{th} (=2.3) deduced[39] for Bi-2:2:1:2, which should be related most directly to γ^{el} because low-frequency ultrasonic waves have very low energy.

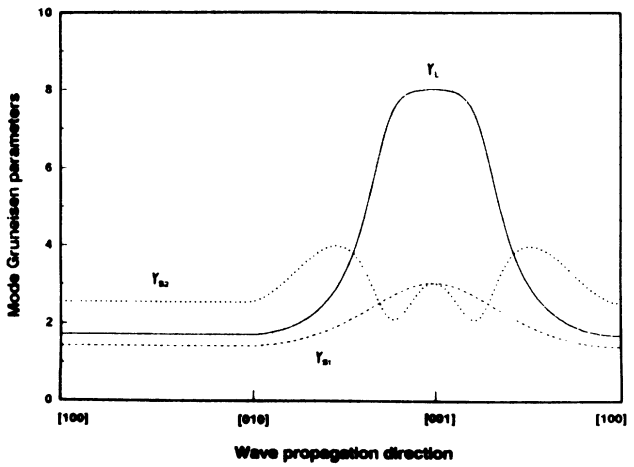

FIG. 8. The directional dependence of the long-wavelength acoustic mode Grüneisen parameters (longitudinal γ_L and shear γ_{S1} and γ_{S2}) of textured Bi-2:2:1:2 at 290 K.

VII. CONCLUSIONS

The velocities of several ultrasonic modes propagated in dense, highly textured Bi-2:2:1:2 ceramic have been measured as functions of temperature between 10 and 290 K and hydrostatic pressure up to 0.15 GPa at 290 K. The data have been used to determine, assuming a structure of cylindrical symmetry, the temperature dependences of the five elastic stiffness tensor components C_{IJ} and of the technologically important quantities, bulk and Young's moduli, and Poisson's ratio. The hydrostatic pressure derivatives $(\partial C_{IJ}/\partial P)_{P=0}$ have been obtained from the variation of sound velocity with pressure. The anisotropy of the elastic and nonlinear acoustic properties has been examined by calculating (i) the cross sections of the three-wave velocity surface and Young's modulus surface and (ii) the linear compressibility and acoustic mode Grüneisen parameters. The physical significance of the results can be summarized as follows.

(i) For textured Bi-2:2:1:2 the elastic stiffness C_{11}, which corresponds to longitudinal wave propagation in the *ab* plane, is much larger than C_{33} associated with such a wave propagated along the *c* axis; this feature is

that found in Brillouin scattering studies of monocrystalline Bi-2:2:1:2.[7] The anisotropy of the stiffness tensor components, which correspond to longitudinal wave propagation along and normal to the forging direction in textured material, is similar in kind to that in single crystals. This behavior is consistent with weaker interlayer binding forces. The elastic stiffnesses C_{11} and C_{44} of textured ceramic are similar to those of monocrystalline Bi-2:2:1:2, while the other C_{IJ} are markedly smaller (Table II), plausibly due to the effects of porosity, microcracks, and microstructural defects in the ceramic.

(ii) The bulk modulus of textured Bi-2:2:1:2 at room temperature and ambient pressure is smaller than that found from very high-pressure x-ray-diffraction measurements of lattice parameters of powdered Bi-2:2:1:2 in diamond anvil cell. This again may be a result of the defective nature of ceramic material.

(iii) The in-plane Young's modulus of both textured and single-crystal Bi-2:2:1:2 is substantially larger than that determined for single-crystal Bi-2:2:1:2 whiskers from static stress-strain measurements. Static tensile tests induce high strains of the order of 1% into materials which probably lead to the small magnitudes of Young's modulus observed for whiskers using this technique.[28]

(iv) Cross sections of the wave velocity surface and Young's modulus surface depict clearly the anisotropy of elastic properties of textured and single-crystal Bi-2:2:1:2. While Young's moduli of textured and monocrystalline Bi-2:2:1:2 are similar in the *ab* plane, the stiffness of the textured material is smaller along the forging direction than that of the crystalline Bi-2:2:1:2; the effect of defects in textured ceramic are more pronounced in the more weakly bound direction normal to the layer planes.

(v) All C_{IJ}, including the bulk and Young's moduli, show a smooth behavior with temperature.

(vi) The pressure derivative $(\partial C_{33}/\partial P)_{P=0}$ of the longitudinal elastic stiffness along the *c* axis is much larger than that $(\partial C_{11}/\partial P)_{P=0}$ in the *ab* plane, as would be expected in a layerlike material with weak interlayer binding forces.

(vii) The linear compression of textured Bi-2:2:1:2 also shows a marked anisotropy: it is larger along the *c* axis than in the *ab* plane.

(viii) There is enhanced anharmonicity for the longitudinal elastic wave propagated along the *c* axis.

ACKNOWLEDGMENTS

We are grateful to the Science and Engineering Research Council (SERC) for financial support. We would like to thank Dr. K. C. Goretta of the Argonne National Laboratory for supplying the textured Bi-2:2:1:2 material and details of its characterization. M. Cankurtaran and G. A. Saunders acknowledge with gratitude North Atlantic Treaty Organization (NATO) Grant No. CRG 891033. Li Jiaqiang also wishes to thank the British Council (Beijing).

*Permanent address: Department of Physics, Hacettepe University, Beytepe, 06532 Ankara, Turkey.

[1]A. Maeda, M. Hase, I. Tsukada, K. Noda, S. Takebayashi, and K. Uchinokura, Phys. Rev. B **41**, 6418 (1990).

[2]D. P. Matheis and R. L. Snyder, Powder Diffr. **5**, 8 (1990).

[3]J. B. Torrance, Y. Tokura, S. J. LaPlaca, T. C. Huang, R. J. Savoy, and A. I. Nazzal, Solid State Commun. **66**, 703 (1988).

[4]P. Bordet, J. J. Capponi, C. Chaillout, J. Chenavas, A. W. Hewat, E. A. Hewat, J. L. Hodeau, M. Marezio, J. L. Tholence, and D. Tranqui, Physica C **156**, 189 (1988).

[5]Y. Wang, J. Wu, J. Zhu, H. Shen, J. Zhang, Y. Yan, and Z. Zhao, Physics Lett. A **142**, 289 (1989).

[6]J. Wu, Y. Wang, H. Shen, J. Zhu, Y. Yan, and Z. Zhao, Phys. Lett. A **148**, 127 (1990).

[7]M. Boekholt, J. V. Harzer, B. Hillebrands, and G. Güntherodt, Physica C **179**, 101 (1991).

[8]C-Y. Chu, J. L. Routbort, Nan Chen, A. C. Biondo, D. S. Kupperman, and K. C. Goretta, Supercond. Sci. Technol. **5**, 306 (1992).

[9]J. Dominec and C. Laermans, Phys. Status Solidi A **135**, K51 (1993).

[10]J. Wu, Y. Wang, P. Guo, H. Shen, Y. Yan, and Z. Zhao, Phys. Rev. B **47**, 2806 (1993).

[11]C. Fanggao, P. J. Ford, G. A. Saunders, L. Jiaqiang, D. P. Almond, B. Chapman, M. Cankurtaran, R. B. Poeppel, and K. C. Goretta, Supercond. Sci. Technol. **6**, 484 (1993).

[12]E. P. Papadakis, J. Acoust. Soc. Am. **42**, 1045 (1967).

[13]E. Kittinger, Ultrasonics **15**, 30 (1977).

[14]R. N. Thurston and K. Brugger, Phys. Rev. **133**, A1604 (1964).

[15]J. Dominec, Supercond. Sci. Technol. **6**, 153 (1993).

[16]T. Yoneda, Y. Mori, Y. Akahama, M. Kobayashi, and H. Kawamura, Jpn. J. Appl. Phys. **29**, L1396 (1990).

[17]M. Cankurtaran, G. A. Saunders, J. R. Willis, A. Al-Kheffaji, and D. P. Almond, Phys. Rev. B **39**, 2872 (1989).

[18]K. C. Goretta, M. E. Loomans, L. J. Martin, J. Joo, R. B. Poeppel, and Nan Chen, Supercond. Sci. Technol. **6**, 282 (1993).

[19]R. H. Arendt, M. F. Garbauskas, C. A. Meyer, F. J. Rotella, J. D. Jorgensen, and R. L. Hitterman, Physica C **182**, 73 (1991).

[20]G. K. White, J. Phys. C **5**, 2731 (1972).

[21]O.-M. Nes, M. Castro, M. Slaski, T. Laegreid, K. Fossheim, N. Motohira, and K. Kitazawa, Supercond. Sci. Technol. **4**, S388 (1991).

[22]C. Fanggao, M. Cankurtaran, G. A. Saunders, D. P. Almond, P. J. Ford, and A. Al-Kheffaji, Supercond. Sci. Technol. **3**, 546 (1990), and references therein.

[23]T. M. Tritt, M. Marone, X.-F. Chen, M. J. Skove, A. C. Ehrlich, G. X. Tessema, D. J. Gillespie, J. P. Franck, and J. Jung, Physica C **178**, 296 (1991).

[24]I. Matsubara, Y. Hashimoto, K. Atago, H. Yamashita, M. Kinoshita, and T. Kawai, Jpn. J. Appl. Phys. **31**, L14 (1992).

[25]J. Turley and G. Sines, J. Phys. D **4**, 264 (1971).

[26]D. J. Gunton and G. A. Saunders, Proc. R. Soc. London, Ser. A **343**, 63 (1975).

[27]X.-D. Xiang, M. Chung, J. M. Brill, S. Hoen, P. Pinsukanjana, and A. Zettl, Solid State Commun. **69**, 833 (1989).

[28]T. M. Tritt, M. Marone, A. C. Ehrlich, M. J. Skove, D. J. Gillespie, R. L. Jacobsen, G. X. Tessema, J. P. Franck, and J.

Jung, Phys. Rev. Lett. **68**, 2531 (1992); R. L. Jacobsen, T. M. Tritt, A. C. Ehrlich, and D. J. Gillespie, Phys. Rev. B **47**, 8312 (1993).
[29]S. J. Collocott and R. Driver, Physica C **167**, 598 (1990).
[30]R. N. Thurston, Proc. IEEE **53**, 1320 (1965).
[31]C. Fanggao, M. Cankurtaran, G. A. Saunders, A. Al-Kheffaji, D. P. Almond, and P. J. Ford, Supercond. Sci. Technol. **4**, 13 (1991).
[32]J. S. Olsen, S. Steenstrup, L. Gerward, and B. Sundqvist, Phys. Scr. **44**, 211 (1991).
[33]F. D. Murnaghan, Proc. Natl. Acad. Sci. USA **30**, 244 (1944).
[34]R. N. Thurston, J. Acoust. Soc. Am. **41**, 1093 (1967).
[35]J. S. Schilling and S. Klotz, in *Physical Properties of High Temperature Superconductors III,* edited by D. M. Ginsberg (World Scientific, Singapore, 1992), p. 59.
[36]W. A. Groen and H. W. Zandbergen, Solid State Commun. **68**, 527 (1989).
[37]K. Brugger, J. Appl. Phys. **36**, 759 (1965); Phys. Rev. **137**, A1826 (1965).
[38]Tu Hailing, G. A. Saunders, W. A. Lambson, and R. S. Feigelson, J. Phys. C **15**, 1399 (1982).
[39]G. K. White, in *Studies of High Temperature Superconductors,* edited by A. Narlikar (Nova Science, New York, 1992), Vol. 9, p. 121.